Smooth Archimedean-spiral ring waveguide for cold atomic gyroscope

Xiaojun Jiang (蒋小军)[1,2], Xiaolin Li (李晓林)[1], Haichao Zhang (张海潮)[1,*], and Yuzhu Wang (王育竹)[1,]**

[1]*Key Laboratory for Quantum Optics and Center for Cold Atom Physics of CAS, Shanghai Institute of Optics and Fine Mechanics, Chinese Academy of Sciences, Shanghai 201800, China*

[2]*University of Chinese Academy of Sciences, Beijing 100049, China*

**Corresponding author: zhanghc@siom.ac.cn; **corresponding author: yzwang@mail.shcnc.ac.cn*

Received January 19, 2016; accepted May 5, 2016; posted online June 1, 2016

We propose a robust scheme that creates a toroidal magnetic potential on a single-layer atom chip. The wire layout consists of two interleaved Archimedean spirals, which avoids the trapping perturbation caused by the input and output ports. By using a rotation bias field, the minimum of the time-averaged orbiting potential is lifted from zero, and then a relatively smooth and harmonic ring trap is formed. The location of the waveguide is immune to the magnetic variations, as it is only determined by the wire layout. The ring waveguide offers an ideal solution to developing a compact and portable atomic gyroscope.

OCIS codes: 020.3320, 020.1335.

doi: 10.3788/COL201614.070201.

There has been widespread interest in developing an atomic gyroscope, as the theoretical sensitivity of an atomic gyroscope corresponds to an improvement by a factor of 10^{10} times greater than a photon-based gyroscope with an equivalent enclosing area[1]. The high sensitivity of an atomic gyroscope is useful for the applications of a rotation sensor[2], general relativity[3], and a fine-structure constant[4,5]. In the last decades, atomic gyroscopes operated in free space have been demonstrated with high sensitivity, showing a short-term rotation-rate sensitivity of 6×10^{-10} rad s^{-1} for one-second measurements[2], and great progress has been made in both theoretical and experimental research[1,6–13]. However, there are several practical challenges to developing a compact and portable rotation sensor device for a real platform, which includes a large-volume system and signal loss that occurs when it experiences rotation[14]. One possible solution is to employ a waveguide. A number of schemes have been proposed for realizing a guided atomic gyroscope[15–17]. With the advantage of the waveguide, the size of the atomic gyroscope can be significantly decreased, and the tolerance to dynamics can be maximized[18]. In addition, a longer interrogation time and larger interferometer areas can be achieved to improve its sensitivity[19]. One of the geometries of interest is the ring waveguide, which provides an ideal geometry for a guided atomic gyroscope sharing identical paths to reject common mode noise[20] and can be created by various methods[21–27]. A ring waveguide on an atom chip is especially suited to fulfilling a compact and portable rotation sensor device. By using chip technology, other optical systems can also be integrated to minimize the volume of the system and increase its functionality at the same time[28–31].

The challenges to realizing a ring waveguide on an atom chip for a guided atomic gyroscope include avoiding the trapping perturbation[32,33] caused by the input and output ports of the rings and creating a non-zero field waveguide at the minimum. When the ultracold atoms propagate through the waveguide and are close to the zero magnetic field points, the atoms confined in the waveguide may be lost by Majorana spin flips into untrapped magnetic substates[34], which limit the sensitivity of the atomic gyroscope due to their short lifetime and low coherence time. To create a non-zero field ring waveguide at the minimum, one way is to use an azimuthal magnetic bias field[32], which can be generated simply by a straight current-carrying wire perpendicular to the chip surface and that passes through the center of the ring waveguide. The challenge is the limited size of the ring waveguide on the chip of just a few millimeters. The other way is to apply a time-averaged orbiting potential (TOP), which is generated by a rapidly oscillating trap field[35]. The TOP technique[34] was used originally to lift the quadrupole trap minimum from zero, which has led to the first observation of a Bose–Einstein condensate (BEC)[36]. By using the TOP technique, a BEC has been produced in a ring waveguide generated by coils[24], in which the time-averaged potential has been generated by varying the currents of the coils.

In this Letter, we propose to investigate a ring waveguide on a single-layer atom chip for a cold atomic gyroscope. The wire configuration is based on an Archimedean spiral[37]. The wire layout avoids the trapping perturbation caused by the input and output ports, resulting in an enclosed guiding loop for neutral atoms in the weak field-seeking states. However, there are two symmetrical zero magnetic field points in the ring waveguide minimum, which is an inherent characteristic of the Archimedean spiral ring magnetic potential. We use a rotation bias field to lift the ring waveguide minimum from zero and smooth the waveguide at the same time. The location

of the waveguide is immune to the magnetic variations, as it is only determined by the wire layout of the atom chip, resulting in a very stable and smooth ring waveguide.

The wire layout to generate the ring potential on the chip is shown in Fig. 1(a). The ring potential is generated by a simple constant current, which is very stable, as the location of the ring potential is only determined by the wire layout of the atom chip. But such a ring potential consists of zero magnetic field points in the minimum, as shown in Fig. 1(b) (red line). It can be seen from Fig. 1(b) that the magnetic field strength of the minimum is equal to the absolute value of the azimuthal angle components of the magnetic field ($B_{\min} = |B_\varphi|$). The reason is that the tangential direction of an arbitrary point $P(r, \varphi, 0)$ in the Archimedean-spiral wires, which represents the direction of the current at point P, is not parallel to the direction of $\mathbf{e}_\varphi$ at point P. The zero magnetic field points are generated as the sign of B_φ changes. The variation of the minimum of magnetic field is about 1 G in Fig. 1(b).

In order to eliminate Majorana spin-flip losses coursed by zero magnetic field points and smooth the minimum of the ring waveguide, we employ a rotation bias field to create a time-orbiting potential trap. In the x–y plane, a rotation bias magnetic field with frequency ω_r is

$$\mathbf{B}_b = B_0[\cos(\omega_r t)\mathbf{e}_x + \sin(\omega_r t)\mathbf{e}_y], \tag{1}$$

where B_0 is the magnitude of the bias field. For further analysis, one can transform the rotation bias magnetic field in the Cartesian coordinate system to the cylindrical coordinate system, and the rotation bias magnetic field is

$$\mathbf{B}_b = B_0[\cos(\omega_r t - \varphi)\mathbf{e}_r + \sin(\omega_r t - \varphi)\mathbf{e}_\varphi]. \tag{2}$$

The magnetic field generated by the wire layout shown in Fig. 1(a) is

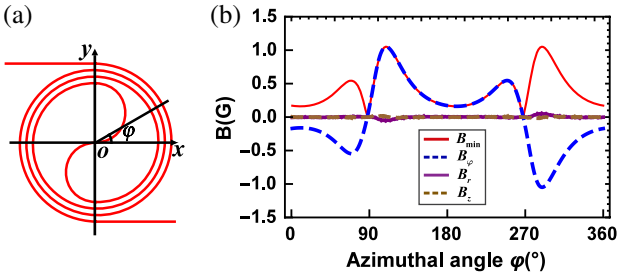

Fig. 1. (a) The wire layout to generate a ring potential on the chip and the definition of the azimuthal angle φ. The radius of the ring potential is 1000 μm and the separation distance between the successive turnings is 110 μm, which determines the height location of the ring potential. (b) The minimum of the magnetic field at a fixed azimuthal angle φ with a dc current of 1 A. $B_{\min}$ (red line) is the magnetic field strength of the minimum. B_r (purple line), B_φ (blue dashed line), and B_z (brown dashed line) are the three components of $B_{\min}$ in the cylindrical coordinate system. The variation of the minimum of the magnetic field is about 1 G.

$$\mathbf{B}_{AS} = B_r\mathbf{e}_r + B_\varphi\mathbf{e}_\varphi + B_z\mathbf{e}_z. \tag{3}$$

With the rotation bias magnetic field, the total magnetic field then becomes

$$\mathbf{B} = \mathbf{B}_{AS} + \mathbf{B}_\mathbf{b}. \tag{4}$$

The magnitude is

$$B(t) = \sqrt{B_z^2 + [B_r + B_0\cos(\omega_r t - \varphi)]^2 + [B_\varphi + B_0\sin(\omega_r t - \varphi)]^2}. \tag{5}$$

To produce a time-averaged potential for the atoms, the rotation frequency ω_r must be higher compared to the trap frequency ω_0 of the atoms. In the meantime, it should be much lower than the Larmor frequency ω_L to prevent the atoms from undergoing a Majorana spin flip into untrapped magnetic sub-states[34]. These two conditions can be summarized as

$$\omega_0 \ll \omega_r \ll \omega_L. \tag{6}$$

For an appropriate value of the rotation frequency ω_r to satisfy the range in Eq. (6), the atoms in the waveguide will experience an effective potential, which is

$$U_{\text{eff}} = \mu_B m_F g_F \frac{\omega_r}{2\pi}\int_0^{2\pi/\omega_r} B(t)\mathrm{d}t, \tag{7}$$

where μ_B refers to the Bohr magneton, m_F is the magnetic quantum number, and g_F is the Lande g-factor.

After applying the rotation bias magnetic field, the minimum of the ring waveguide is non-zero and the ring waveguide is smoothed, as shown in Fig. 2, where the magnitude B_0 is 2 G. The fluctuation appears on the area of $\varphi = 90°$ to $\varphi = 120°$ and $\varphi = 270°$ to $\varphi = 300°$. The maximum value of the minimum is 2.14 G at $\varphi = 109°$ and $\varphi = 289°$. So the variation of the minimum of the magnetic field is reduced to 0.14 G. For ^{87}Rb atoms in the $|F = 2, m_F = 2\rangle$ ground state, the potential barrier is about 9.38 μK. To ensure that the cold atoms pass

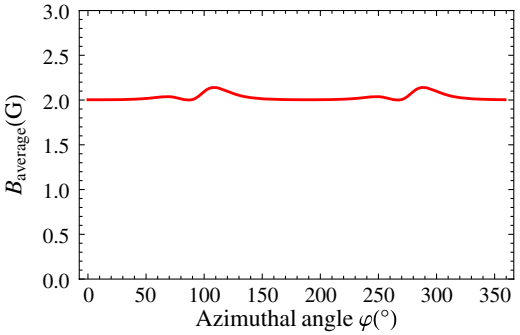

Fig. 2. Time-averaged magnetic field of the minimum at a fixed azimuthal angle φ with a rotation bias magnetic field. The magnitude of the bias magnetic field is 2 G. The variation of the minimum of magnetic field is 0.14 G.

through the potential barrier, one can employee a large-momentum transfer scheme[38,39] to split the atoms or load the atoms[27,29] near $\varphi = 109°$, where the potential has the maximum value.

Figure 3 plots the locus of the position of the instantaneous zero magnetic field point, which is known as the circle of death. It shows that there are two circles (blue lines) around the minimum of the ring waveguide (red line). The distance between the circle of death and the ring waveguide, which can be defined as the radius of death, is about 10 μm. When the cold atoms or BEC move into the two circles, the atoms may be lost from the waveguide due to the Majorana spin flips. In addition, the position of the ring waveguide is independent of the rotation bias field.

To further illuminate the time-averaged potential, we investigate the value of magnitude B_0. According to Eq. (5), at the minimum point (r_0, φ_0, z_0), $B_{r_0} = 0$ and $B_{z_0} = 0$, and the magnetic field is

$$B(r_0, \varphi_0, z_0, t) = \sqrt{B_{\varphi_0}^2 + B_0^2 + 2B_{\varphi_0}B_0 \sin(\omega_r t - \varphi_0)}. \tag{8}$$

In order to make sure the instant value of the magnetic field at any time is non-zero at the minimum point, which means the circle of death does not intersect with the ring waveguide at any point, the magnitude B_0 should be chosen to be larger than the maximum value of $B_{\min}$.

Figure 4 shows the variation of the characteristics of the time-averaged potential as a function of the magnitude B_0. It can be seen that the radius r_D increases as B_0 increases, while the variation δB, gradient B'_z, and the depth U_D decrease as B_0 increases. The radius r_D should be chosen to be larger than the radius of the cold atoms. The variation δB can be reduced by increasing B_0. The factors to determine the upper limit of B_0 are the gradient B'_z and the depth U_D. For ^{87}Rb atoms, the gradient B'_z should be chosen to be larger than 15.5 G/cm to overcome the gravity. To prevent the cold atoms boiling out of the trap, the depth U_D should be 5 to 7 times larger than the mean atomic energy[40]. For ultracold atoms under the temperature 300 nK, the depth U_D should be larger than 1.5 μK. From Fig. 4, we can see that the magnitude B_0 should be less than 3.8 G. The optimal value of B_0 can be chosen as 3 G, where the radius r_D is about 20 μm and the variation δB is less than 0.1 G. The depth $U_D =$ 1.9 μK is sufficiently deep for ultracold atoms under temperature 300 nK. For ^{87}Rb atoms in the $|F = 2, m_F = 2\rangle$ ground state, the trapping frequency of time-averaged potential is reduced to $\omega_r = 2\pi \times 6$ kHz and $\omega_z = 2\pi \times 7$ kHz.

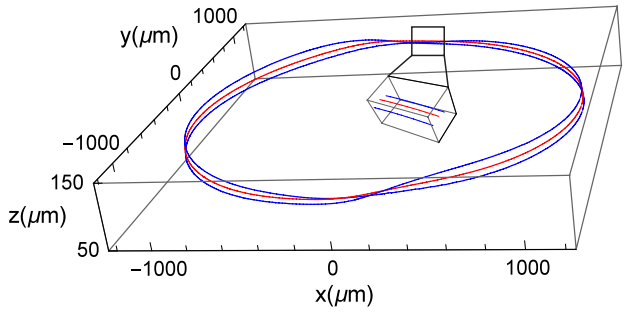

Fig. 3. Locus of the position of the instantaneous zero points (blue lines), known as the circle of death, and the time-averaged minimum points (red line). The circles of death are two circles around the minimum of the ring waveguide. The image in the center shows a zoomed-in view of a slice of the circles of death. The radius of death is about 10 μm.

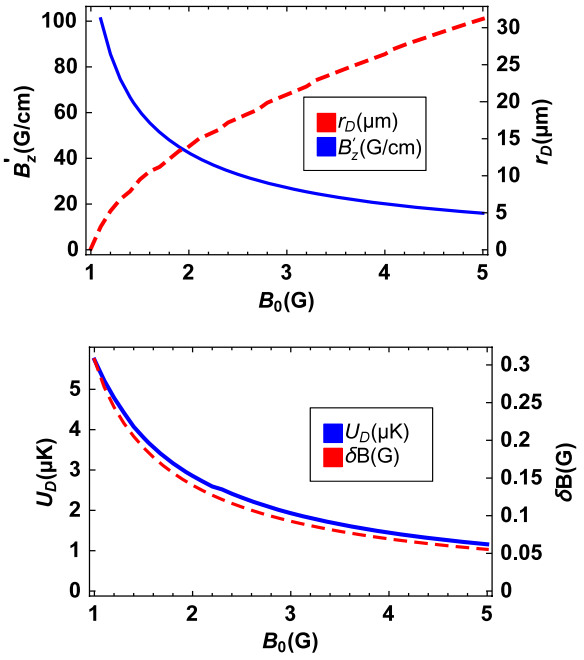

Fig. 4. Variation of the characteristics of the time-averaged potential as a function of the magnitude of the bias field B_0. (a) The filed gradient in the z direction (blue line) and the radius of death (red dashed line) are represented by B'_z and r_D, respectively. (b) The trap of depth (blue line) and the variation of the minimum of magnetic field (red dashed line) are represented by U_D and δB, respectively.

We will now briefly discuss the experimental scheme for the atomic gyroscope on the atom chip. After evaporative cooling, the cold atoms or BEC are loaded into the ring waveguide[29], and a sequence of two standing-wave square pulses are applied to split the cold atoms into two symmetrical parts with a well-defined initial momentum[41]. Subsequently, the two symmetrical parts start to freely propagate in the ring waveguide in opposite directions. When the atoms return to the loading point, a second double-square-pulse beam splitter is applied to recombine the two parts. Then we can detect the number of atoms that carry a phase shift to measure the rotation.

In conclusion, we propose a scheme to create a ring waveguide based on Archimedean-spiral wires on an atom chip for an atomic gyroscope. The Archimedean-spiral wires can create an enclosed ring waveguide which avoids the trapping perturbation caused by the input and output ports. With a rotation bias field, a time-averaged

potential is created to lift the minimum of the ring waveguide from zero and smooth the minimum. The location of the ring waveguide on the atom chip is only determined by the wire layout. The optimal value of 3 G of the bias magnetic field is obtained, which keeps the waveguide smooth and sufficiently deep for ultracold atoms. The Archimedean-spiral ring waveguide offers the prospect of developing a compact and portable atomic gyroscope.

This work was supported by the State Key Basic Research Program (No. 2001CB309307) and the National Natural Science Foundation of China (Nos. 10974210 and 10474105).

References

1. T. L. Gustavson, P. Bouyer, and M. A. Kasevich, Phys. Rev. Lett. **78**, 2046 (1997).
2. T. L. Gustavson, A. Landragin, and M. A. Kasevich, Class. Quantum Grav. **17**, 2385 (2000).
3. C. M. Will, Living Rev. Relativ. **9**, 3 (2006).
4. A. Wicht, J. M. Hensley, E. Sarajlic, and S. Chu, Phys. Scr. **T102**, 82 (2002).
5. S. Gupta, K. Dieckmann, Z. Hadzibabic, and D. E. Pritchard, Phys. Rev. Lett. **89**, 140401 (2002).
6. M. K. Oberthaler, S. Bernet, E. M. Rasel, J. Schmiedmayer, and A. Zeilinger, Phys. Rev. A **54**, 3165 (1996).
7. D. S. Durfee, Y. K. Shaham, and M. A. Kasevich, Phys. Rev. Lett. **97**, 240801 (2006).
8. B. Canuel, F. Leduc, D. Holleville, A. Gauguet, J. Fils, A. Virdis, A. Clairon, N. Dimarcq, C. H. J. Bordé, A. Landragin, and P. Bouyer, Phys. Rev. Lett. **97**, 010402 (2006).
9. S. M. Dickerson, J. M. Hogan, A. Sugarbaker, D. M. Johnson, and M. A. Kasevich, Phys. Rev. Lett. **111**, 083001 (2013).
10. G. Tackmann, P. Berg, S. Abend, C. Schubert, W. Ertmer, and E. M. Rasel, C. R. Phys. **15**, 884 (2014).
11. A. V. Rakholia, H. J. McGuinness, and G. W. Biedermann, Phys. Rev. Appl. **2**, 054012 (2014).
12. B. Estey, C. H. Yu, H. Müller, P. C. Kuan, and S. Y. Lan, Phys. Rev. Lett. **115**, 083002 (2015).
13. X. Li, W. Ling, Y. Wei, and Z. Xu, Chin. Opt. Lett. **13**, 090603 (2015).
14. G. Tackmann, P. Berg, C. Schubert, S. Abend, M. Gilowski, W. Ertmer, and E. M. Rasel, New J. Phys. **14**, 015002 (2012).
15. R. Franzosi, B. Zambon, and E. Arimondo, Phys. Rev. A **70**, 053603 (2004).
16. J. H. T. Burke, B. Deissler, K. J. Hughes, and C. A. Sackett, Phys. Rev. A **78**, 023619 (2008).
17. H. Yan, Appl. Phys. Lett. **101**, 194102 (2012).
18. J. H. Burke, Proc. SPIE **9378**, 93781Z (2015).
19. B. Barrett, R. Geiger, I. Dutta, M. Meunier, B. Canuel, A. Gauguet, P. Bouyer, and A. C. R. Landragin, C. R. Phys. **15**, 875 (2014).
20. S. Wu, E. Su, and M. Prentiss, Phys. Rev. Lett. **99**, 173201 (2007).
21. I. Lesanovsky and W. V. Klitzing, Phys. Rev. Lett. **99**, 083001 (2007).
22. A. D. West, C. G. Wade, K. J. Weatherill, and I. G. Hughes, Appl. Phys. Lett. **101**, 023115 (2012).
23. J. A. Sauer, M. D. Barrett, and M. S. Chapman, Phys. Rev. Lett. **87**, 270401 (2001).
24. S. Gupta, K. W. Murch, K. L. Moore, T. P. Purdy, and D. M. Stamper-Kurn, Phys. Rev. Lett. **95**, 143201 (2005).
25. A. S. Arnold, C. S. Garvie, and E. Riis, Phys. Rev. A **73**, 041606 (2006).
26. P. F. Griffin, E. Riis, and A. S. Arnold, Phys. Rev. A **77**, 051402R (2008).
27. J. D. Pritchard, A. N. Dinkelaker, A. S. Arnold, P. F. Griffin, and E. Riis, New J. Phys. **14**, 103047 (2012).
28. M. Yun and J. Yin, Chin. Opt. Lett. **3**, 125 (2005).
29. J. Fortágh and C. Zimmermann, Rev. Mod. Phys. **79**, 235 (2007).
30. A. Cronin, J. Schmiedmayer, and D. E. Pritchard, Rev. Mod. Phys. **81**, 1051 (2009).
31. W. Yang, L. Zhou, S. Long, W. Peng, J. Wang, and M. Zhan, Chin. Opt. Lett. **13**, 011401 (2015).
32. P. M. Baker, J. A. Stickney, M. B. Squires, J. A. Scoville, E. J. Carlson, W. R. Buchwald, and S. M. Miller, Phys. Rev. A **80**, 063615 (2009).
33. M. B. Crookston, P. M. Baker, and M. P. Robinson, J. Phys. B: At. Mol. Opt. Phys. **38**, 3289 (2005).
34. W. Petrich, M. H. Anderson, J. R. Ensher, and E. A. Cornell, Phys. Rev. Lett. **74**, 3352 (1995).
35. A. S. Arnold, J. Phys. B **37**, L29 (2004).
36. M. H. Anderson, J. R. Ensher, M. R. Matthews, C. E. Wieman, and E. A. Cornell, Science **269**, 198 (1995).
37. X. J. Jiang, X. L. Li, X. P. Xu, H. C. Zhang, and Y. Z. Wang, Chin. Phys. Lett. **32**, 020301 (2015).
38. H. Müller, S.-W. Chiow, Q. Long, S. Herrmann, and S. Chu, Phys. Rev. Lett. **100**, 180405 (2008).
39. G. D. McDonald, C. C. N. Kuhn, S. Bennetts, J. E. Debs, K. S. Hardman, M. Johnsson, J. D. Close, and N. P. Robins, Physica Rev. A **88**, 053620 (2013).
40. J. Reichel, Appl. Phys. B **74**, 469 (2002).
41. S. Wu, Y. J. Wang, Q. Diot, and M. Prentiss, Phys. Rev. A **71**, 043602 (2005).